CONTRACTOR REPORT

NASA CR-1508

c. 1

RESEARCHES IN OPTIMAL RENDEZVOUS

by Walter Heine

Prepared by
STANFORD UNIVERSITY
Stanford, Calif.
for

NATIONAL AERONAUTICS AND SPACE ADMINISTRATION • WASHINGTON, D. C. • FEBRUARY 1970

NASA CR-1508

RESEARCHES IN OPTIMAL RENDEZVOUS

By Walter Heine

Issued by Originator as SUDAAR No. 382

Prepared under Grant No. NGR-05-020-007 by
STANFORD UNIVERSITY
Stanford, Calif.

for

NATIONAL AERONAUTICS AND SPACE ADMINISTRATION.

For sale by the Clearinghouse for Federal Scientific and Technical Information
Springfield, Virginia 22151 – Price $3.00

ABSTRACT

This research is concerned with the time-fixed transfer between two elliptic orbits. The transfer is to be accomplished with minimum fuel requirements. Impulsive thrusts are assumed. The objective of the problem is to determine the number and nature of the impulses required for various orbit geometries. Two special cases are investigated which result from assuming symmetric impulse magnitude and locations. The first case has symmetry about the line of nodes and the second has symmetry about a line perpendicular to the line of nodes. The assumption of symmetry of the impulses requires that the orbits, assumed to be nearly circular, have equal semi-major axes. The application of symmetric impulses causes the vacant focus to be displaced perpendicular to the line of symmetry. The maximum number of impulses in the first case is six, whereas in the second the maximum number is four. Charts are presented, for both cases of the time-fixed transfer problem, which show the definition of one, two, three, four, five, and six impulse regions in parameter space.

CONTENTS

ILLUSTRATIONS

Chapter I

INTRODUCTION

This research is concerned with the time-fixed transfer between two elliptic orbits. The transfer is to be accomplished with minimum fuel requirements. Impulsive thrusts are used which have been shown to give optimal solutions for most cases of time-fixed transfer.

In the last ten years much study has been devoted to the problem of optimal transfer. However, the first investigation was made much earlier by Hohmann [1] in 1925. Hohmann first considered the problem of applying two impulsive thrusts to effect a transfer between coplanar circular orbits. The impulses were found to be applied at the apses of the transfer orbit and directed tangentially. This strategy is the well-known Hohmann transfer.

Many important results have been obtained for optimal multiple-impulse transfer. In the last decade Lawden [2,3,4], Breakwell [9,10, 11], and others have made many publications in optimal transfer theory. Hoelker and Silber [5] and Shternfeld [6] investigated the possibility of three impulse for transfer between coplanar circular orbits. Optimal transfers were found to be two impulse, three impulse or bi-parabolic in [5], [6], and by Edelbaum [7]. Marchal [8] has presented the most comprehensive discussion of this problem in 1965. Winn [12] has investigated optimal transfers between coaxial ellipses. Both Marec [13] and Edelbaum [14] have considered optimal transfer in the vicinity of a circular orbit. Kuzmak [15] used Lagrange's method in connection with this problem. Some numerical results were obtained by Eckel [16].

For time-fixed transfers theoretical studies have been made by Lawden [4] and Lion and Handelsmann[17]. Marec [18] has extended his work on transfer analysis to include time-fixed rendezvous of long duration. Gobetz and Doll [19,20] have investigated the rendezvous problem in the light of interplanetary mission planning. Prussing [21] has made investigations of coplanar, circular orbit rendezvous. Kolbe and Sagirow [22] and Marinescu [23] have also made investigations in the

rendezvous problem but with different cost functions and, in the case of Marinescu, in low thrust applications.

The method and results in the determination of optimal impulsive space maneuvers have been surveyed by Marchal, Marec, and Winn [24] and by Robinson [25].

A general analysis of the time-fixed transfer or rendezvous problem is presented in Chapter II. The objective of the time-fixed problem is to determine the number and nature of the impulses required for various orbit geometries. Two special cases are investigated which result from assuming symmetric impulse magnitudes and locations. The first case has symmetry about the line of nodes, discussed in Chapter III, and the second has symmetry about a line perpendicular to the line of nodes, also discussed in Chapter III. The assumption of symmetry of the impulses yields the result that the orbits, initially assumed to be nearly circular, now also have equal semi-major axes due to the motion of the vacant focus. The method used in the entire time-fixed analysis follows Prussing [21].

The maximum number of impulses was found to be six. Charts are presented, for both cases, which show the definition of the one, two, three, four, five, and six impulse regions in the space of $(\theta_f - \theta_o)$ and the two ratios of the orbit parameters Δe, Δi, and a phasing parameter $\Delta\theta'$.

Chapter IV presents the conclusions of the results obtained and gives recommendations for future research.

Chapter II

GENERAL ANALYSIS OF RENDEZVOUS OR TIME-FIXED TRANSFER PROBLEM

The problem of optimal rendezvous is of practical importance. The analysis presented in this chapter is concerned with the time-fixed rendezvous between neighboring, non-coplanar, elliptical orbits. For an orbital rendezvous the desired final boundary conditions require that the position and velocity of the vehicle at the final time be the position and velocity of the target body. Optimal solutions to time-free transfer require less restrictive final boundary conditions. The analysis follows from Prussing's [21] presentation of a similar problem.

A. Analysis

Since a thrusting vehicle is assumed to be moving in a gravitational field, the equations of motion can be written, using a state vector form, where

$$\bar{x} = \begin{bmatrix} \bar{r} \\ \bar{v} \end{bmatrix} \tag{2.1}$$

as

$$\dot{\bar{x}} = \bar{f}(\vec{x}, \bar{a}) \ . \tag{2.2}$$

The cost for the rendezvous problem is given by

$$\phi = -\int_{t_o}^{t_f} |a| \ dt \tag{2.3}$$

or

$$\dot{\phi} = -a \ . \tag{2.4}$$

The negative sign appears so that the maximum principle can be used, that is, maximizing the cost ϕ given by (2.3) minimizes the fuel requirements.

The Hamiltonian

$$H = \bar{\lambda}^T f \tag{2.5}$$

is given, after augmenting the states to include ϕ and using the fact that $\lambda_p = -1$, by

$$H = \bar{\lambda}_r \cdot \bar{v} + \lambda_v \cdot \bar{g} + \bar{\lambda}_v \cdot \bar{a} - a \ . \tag{2.6}$$

The control in this problem is the thrust direction and magnitude. Applying Pontryagin's maximum principle yields:

$$\max_{\bar{a}} H \Longrightarrow \bar{\lambda}_v \cdot \bar{a} = |\bar{\lambda}_v| \ a \ . \tag{2.7}$$

This states that the optimal $\bar{a}$ is parallel to $\bar{\lambda}_v$, since the dot product is maximum when two vectors being so multiplied are parallel.

Substituting (2.7) back into (2.6) gives

$$H = \bar{\lambda}_r \cdot \bar{v} + \bar{\lambda}_v \cdot \bar{g} + (|\bar{\lambda}_v| - 1) \ a \ . \tag{2.8}$$

Maximizing the Hamiltonian with respect to the magnitude of a row yields:

$$|\bar{\lambda}_v| > 1 \Longrightarrow \text{maximum} \quad a$$

$$|\bar{\lambda}_v| < 1 \Longrightarrow a = 0$$

$$|\bar{\lambda}_v| = 1 \Longrightarrow \text{unknown} \quad a \ . \tag{2.9}$$

If unlimited power is assumed so that impulsive thrusts are now acceptable, then for $|\bar{\lambda}_v| > 1$ an infinite thrust will be used for a finite length of time. This would definitely not minimize the cost, so that in this analyziz, $|\bar{\lambda}_v|$ can never be greater than unity. For $|\bar{\lambda}_v|$ identically equal to unity an impulsive type thrust can be applied since, generally, $|\bar{\lambda}_v| = 1$ only instantaneously, except in a singular case where $|\bar{\lambda}_v| = 1$ always. Therefore the impulsive thrusts occur when

$$|\bar{\lambda}_v| = 1$$

and have a direction given by

$$\frac{\bar{a}}{a} = \bar{\lambda}_v \ .$$

In addition, the primer vector, $\bar{\lambda}_v$, and its first derivatives must be continuous.

Summarizing, the necessary conditions for an optimal impulse rendezvous are:

(1) $\bar{\lambda}_v$, which Lawden [4] calls the primer vector, and its first derivative must be continuous everywhere,

(2) The thrust impulses are to be applied in the direction of the primer vector at the times for which $|\bar{\lambda}_v| = 1$,

(3) $|\bar{\lambda}_v| \leq 1$ during the transfer,

(4) From conditions 1 and 3 the slope of the primer magnitude time history is horizontal for impulses which are not at the initial and final times.

These conditions are seen more clearly in Fig. 1 which shows a typical time history for an optimal three-impulse solution.

In analyzing optimal finite thrust boundary value problems a primer history can be found in terms of the optimal thrust magnitude which will

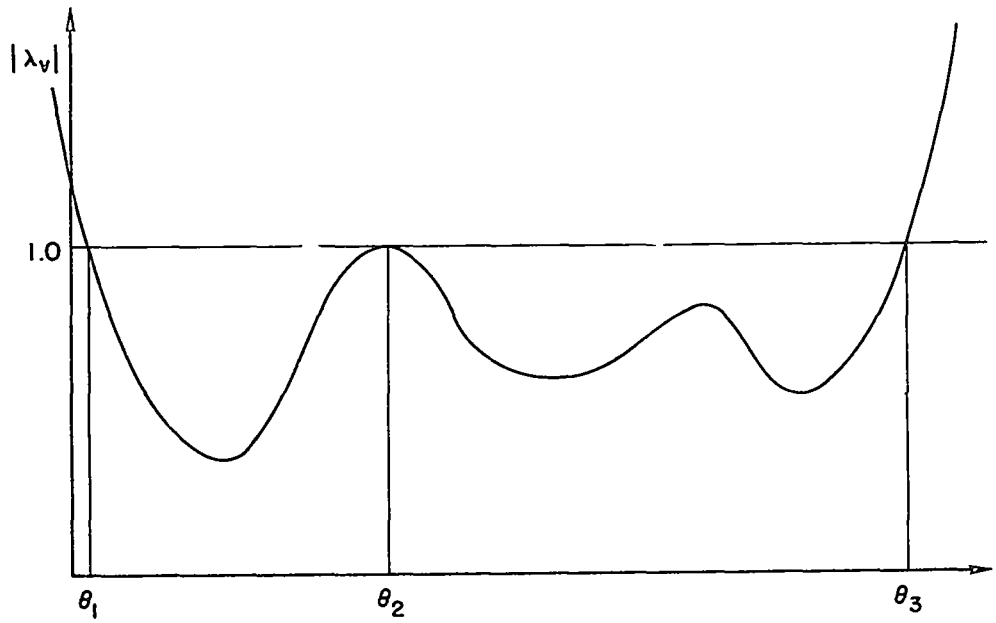

Fig. 1. TYPICAL THREE IMPULSE, PRIMER MAGNITUDE TIME HISTORY.

satisfy the boundary conditions with no restriction on the primer magnitude. However, for impulsive thrusts the magnitude of the primer is constrained to less than or equal to unity. In the general problem the primer history is dependent on the thrust magnitude. By assuming small orbit changes and retaining only first-order terms in an expansion, this dependency is removed. Thus linearizing the equations of motion about a circular reference orbit, the well-known Hill's equations are obtained as

$$\begin{aligned}
\dot{x} &= u \\
\dot{y} &= v \\
\dot{z} &= w \\
\dot{u} &= f_x + 2nv + 3n^2x \\
\dot{v} &= f_y - 2nu \\
\dot{w} &= f_z - n^2z
\end{aligned} \tag{2.10}$$

where x is the radial component, y is the circumferential component, and z is the out-of-plane component; f_x, f_y, and f_z are the corresponding thrust components and n is the mean motion. Equation (2.10) can be rewritten as

$$\dot{X} = FX + GU \tag{2.11}$$

where

$$X = \begin{bmatrix} x \\ y \\ z \\ u \\ v \\ w \end{bmatrix}$$

$$F = \begin{bmatrix} 0 & 0 & 0 & 1 & 0 & 0 \\ 0 & 0 & 0 & 0 & 1 & 0 \\ 0 & 0 & 0 & 0 & 0 & 1 \\ 3n^2 & 0 & 0 & 0 & 2n & 0 \\ 0 & 0 & 0 & -2n & 0 & 0 \\ 0 & 0 & 0 & 0 & 0 & n^2 \end{bmatrix}$$

$$G = \begin{bmatrix} \bar{0}_3 & & \bar{0}_3 & \\ & 1 & 0 & 0 \\ \bar{0}_3 & 0 & 1 & 0 \\ & 0 & 0 & 1 \end{bmatrix} \tag{2.12}$$

$$U = \begin{bmatrix} \bar{0}_1 \\ f_x \\ f_y \\ f_z \end{bmatrix}$$

where

$$\bar{0}_3 \begin{bmatrix} 0 & 0 & 0 \\ 0 & 0 & 0 \\ 0 & 0 & 0 \end{bmatrix} \qquad \bar{0}_1 = \begin{bmatrix} 0 \\ 0 \\ 0 \end{bmatrix} . \tag{2.13}$$

The effect of several velocity changes, due to the impulsive thrusts, during a transfer is obtained by superposition of the solutions of the linearized equations of motion (2.11). In terms of velocity changes made at times $t_j (j = 1, \ldots, n)$ the final state is given by

$$X(t_f) = \Phi(t_f, t_o)\, X(t_o) + \sum_{j=1}^{n} \Phi(t_f, t_j) \begin{bmatrix} \bar{0}_1 \\ \Delta V_j \end{bmatrix} \tag{2.14}$$

where $X(t_o)$ is the final state and $\Phi(t_i, t_j)$ is the state transition matrix with units chosen such that R, the radius of the reference orbit, and n, the mean motion of the reference orbit, are both unity. The transition matrix is given by

$$\Phi(t_i, t_j) = \begin{bmatrix} 4-3\cos\theta & 0 & 0 & \sin\theta & 2(1-\cos\theta) & 0 \\ 6(\sin\theta-\theta) & 1 & 0 & 2(\cos\theta-1) & 4\sin\theta-3\theta & 0 \\ 0 & 0 & \cos\theta & 0 & 0 & \sin\theta \\ 3\sin\theta & 0 & 0 & \cos\theta & 2\sin\theta & 0 \\ 6(\cos\theta-1) & 0 & 0 & -2\sin\theta & 4\cos\theta-3 & 0 \\ 0 & 0 & -\sin\theta & 0 & 0 & \cos\theta \end{bmatrix} \tag{2.15}$$

where $\theta = n(t_i - t_j)$.

For convenience a new final state variable is defined as

$$X'(t_f) = X(t_f) - \Phi(t_f, t_o)\, X(t_o) \tag{2.16}$$

and the transition matrix under the summation is partitioned so that

$$\Phi(t_f, t_j) = [\Phi_1(t_f, t_j) \vdots \Phi_2(t_f, t_j)] \ . \tag{2.17}$$

Substituting (2.16) and (2.17) into (2.14) yields:

$$X(t_f) = \sum_{j=1}^{n} \Phi_2(t_f, t_j)\, \overline{\Delta V}_j \ . \tag{2.18}$$

At the time of the impulse the magnitude of the primer vector is unity and its direction is identical to the direction of the thrust so that

$$(\lambda_v)_j = \frac{\overline{\Delta V}_j}{|\Delta V_j|} \ . \tag{2.19}$$

In terms of $\bar{\lambda}_v$ and the definition

$$\Psi_j = \Phi_2(t_f, t_j)(\overline{\lambda_v})_j \tag{2.20}$$

Eq. (2.18) becomes

$$X'(t_f) = \sum_j \Psi(t_j, (\bar{\lambda}_v)_j)\ |\overline{\Delta V}_j| \tag{2.21}$$

where

$$\Psi(t_j, (\bar{\lambda}_v)_j) = [\bar{\Psi}_1, \bar{\Psi}_2, \ldots, \bar{\Psi}_n]$$

$$\overline{\Delta V} = \begin{bmatrix} \Delta V_1 \\ \Delta V_2 \\ \vdots \\ \Delta V_n \end{bmatrix} . \tag{2.22}$$

The arguments of the six-vector $\Psi(t_j, (\bar{\lambda}_v)_j)$ are determined from a knowledge of the primer vector. The t_j's are determined when the magnitude of the primer is unity and the components of the $(\bar{\lambda}_v)_j$'s are the direction cosines $(\lambda_u)_j$, $(\lambda_v)_j$, and $(\lambda_w)_j$. The six-vector $\bar{\Psi}_j$ has the physical interpretation of being the change in the final state due to a unit magnitude velocity change at time t_j in the optimal direction $\bar{\lambda}_v(t_j)$.

Combining (2.5) and (2.10) gives the Hamiltonian as

$$\begin{aligned} H = {} & \lambda_x u + \lambda_y v + \lambda_z w \\ & + \lambda_u (f_x + 2nv + 3n^2 x) \\ & + \lambda_v (f_y - 2nu) + \lambda_w (f_z - n^2 z) - a . \end{aligned} \tag{2.23}$$

The adjoint satisfies the differential equation

$$\dot{\lambda}_x^T = -H_x . \tag{2.24}$$

Equation (2.23) together with (2.24) yield:

$$\ddot{\lambda}_u = 3n^2\lambda_u + 2n\lambda_v$$

$$\ddot{\lambda}_v = -2n\lambda_u$$

$$\ddot{\lambda}_w = -n^2\lambda_w \cdot \tag{2.25}$$

The out-of-plane component is uncoupled from the other components and satisfies a linear oscillator equation. The in-plane components are solved simultaneously and the solutions are

$$\lambda_u = 2A + B\cos\theta$$

$$\lambda_v = -3A\theta - E - 2B\sin\theta$$

$$\lambda_w = M\cos\theta + N\sin\theta \tag{2.26}$$

where $\theta = n(t - t_p)$ and A, B, E, M, N, and t_p are constants of integration. Equation (2.26) may also be obtained by a linear combination of the rows of the last three columns of (2.15) since

$$(\bar{\lambda}_r^T(t), \bar{\lambda}_v^T(t)) = (\bar{\lambda}_r^T(t_f), \bar{\lambda}_v^T(t_f))\,\Phi(t_f, t)\,. \tag{2.27}$$

Impulses are applied when $|\bar{\lambda}_v| = 1$ so that the remaining Hamiltonian is now

$$H = \bar{\lambda}_r \cdot \bar{v} + \bar{\lambda}_v \cdot \bar{g} = \bar{\lambda}_r \cdot \bar{v} - n^2\bar{\lambda}_v \cdot \bar{r}\,. \tag{2.28}$$

This can be rewritten as

$$H = -na(\dot{\lambda}_v + n\lambda_u) - n^2a\lambda_u\,. \tag{2.29}$$

From the expressions for λ_u and λ_v, (2.26), the Hamiltonian is now

$$H = -n^2 aA \quad . \tag{2.30}$$

For time-free transfer $H = 0$, which implies that time-free transfer is obtained here for $A = 0$.

From (2.26) it is evident that for the linearized equations of motion the primer vector, evaluated along the circular reference orbit, is independent of the perturbed trajectory. Thus the linearized equations of motion and the adjoint equations can be solved separately. This is in contrast to a problem with a nonlinear state equation in which the adjoint variables are functions of the states. Because of this separability the matrix Ψ can be determined from the necessary conditions for an optimal solution independent of the boundary value problem. And since the primer vector is not a function of the states it is continuous along with its first derivative.

The solution to the rendezvous problem requires more than a knowledge of thrust magnitude, direction, and location. For an initial location of the target, the number of impulses to realize the optimal rendezvous must be determined. The number depends on the transfer time. The problem is further complicated in that for a fixed transfer time and initial conditions, either an initial or final coast period may be required in the optimal solution.

For impulsive solutions to transfer problems Neustadt [27] and Potter [28] have found that for a linear system the maximum number of impulses necessary to realize the optimum transfer is equal to the number of constraints on the state variables at the specified final time. They show that any velocity impulse schedule containing a larger number of impulses than the number of constraints can be reduced to an impulse schedule with the number of impulses equaling the number of constraints without increasing the total impulse magnitude required. Here, in the non-coplanar problem, three position and three velocity constraints exist at the final time, thus the maximum number of impulses required is

six. Another result of Neustadt [27] is a theorem that guarantees the absence of local false maxima. Hence, a Hamiltonian that provides a solution to the rendezvous boundary value problem automatically provides a globally optimal solution.

Since the amount of fuel consumed depends greatly on the position of the target relative to the rendezvous vehicle at launch, a certain amount of the specified transfer time in some cases is best invested in a coast period, allowing a geometrically more favorable rendezvous. An initial coast implies waiting in the initial orbit before applying the first thrust impulse. A final coast implies that the rendezvous takes place earlier than the specified final time. A combination of initial and final coast is often optimal.

To illustrate the rendezvous requiring coasting periods to yield optimal solutions, consider the primer magnitude shown in Fig. 2. Impulses are applied whenever $|\bar{\lambda}_v| = 1$ so that in this case they occur

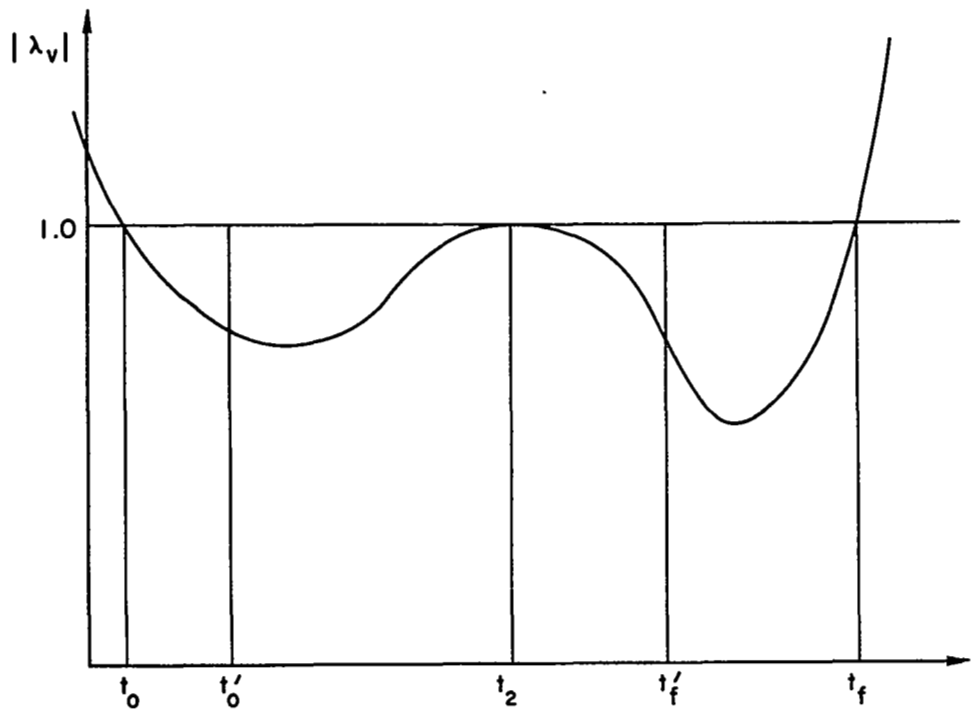

Fig. 2. PRIMER MAGNITUDE SHOWING COAST PERIODS.

at $t = t_o, t_1, t_f$. The total transfer time being $t_f - t_o$. If, however, the final time were to occur at some t_f' less than t_f but greater than t_2, impulses would be applied at $t = t_o$ and t_1. Since $|\bar{\lambda}_v|$ has not yet become one at $t = t_f'$ no other impulses are required so that rendezvous is achieved at $t = t_2$, followed by a coast in the final orbit from t_2 to t_f' so that the total transfer time $t_f' - t_o$ is satisfied. An initial coast would occur for an initial time t_o' greater than t_o but less than t_2. Here the coast would be in the initial orbit from t_o' to t_2 followed by two impulses at t_2 and t_f with rendezvous being achieved at $t = t_f$.

B. Determination of Optimal Impulse Solutions

The magnitude of the primer is given as

$$|\bar{\lambda}_v| = \sqrt{\lambda_u^2 + \lambda_v^2 + \lambda_w^2} \quad . \tag{2.31}$$

Substituting (2.27) and normalizing with respect to one of the constants of integration, say B, yields

$$\frac{|\bar{\lambda}_v|^2}{B^2} = (2\gamma + \cos\theta)^2 + [3\gamma(\theta + \eta) + 2\sin\theta]^2$$

$$+ (\mu\cos\theta + \zeta\sin\theta)^2 \tag{2.32}$$

where the four parameters are

$$\gamma = \frac{A}{B}$$

$$\eta = \frac{E}{3\gamma B}$$

$$\mu = \frac{M}{B}$$

$$\zeta = \frac{N}{B} \ . \tag{2.33}$$

The location of the maxima are the θ's that satisfy

$$\frac{d}{d\theta}\left(\frac{|\bar{\lambda}_v|^2}{B^2}\right) = 0 \tag{2.34}$$

or the transcendental equation

$$2\gamma(\theta + \eta) = -\frac{\sin\theta\left(\frac{4}{3}\gamma + \cos\theta\right)}{\frac{3}{2} + \cos\theta} + \frac{(\mu \sin\theta - \zeta\cos\theta)(\mu\cos\theta + \zeta\sin\theta)}{3\left(\frac{3}{2}\gamma + \cos\theta\right)} \ . \tag{2.35}$$

For more than three impulses there must exist at least $(i - 2)$ equal maxima where i is four, five, or six corresponding to the number of impulses. Therefore, for six impulses there must exist a θ_1, θ_2, θ_3, and θ_4, all of which must satisfy (2.35) and simultaneously satisfy

$$F(\theta_1) = F(\theta_2) = F(\theta_3) = F(\theta_4) \tag{2.36}$$

where

$$F(\theta_i) = \left.\frac{|\bar{\lambda}_v|^2}{B^2}\right|_{\theta = \theta_i} \qquad (i = 1, 2, 3, 4) \ .$$

In the general problem the number of free variables that are present is six, that is, γ, μ, ζ, η, t_p, and the impulse magnitude $|\overline{\Delta V}_j|$. For one impulse transfer the five parameters plus one impulse magnitude constitute the six free variables. Two impulses would require a constraint on the magnitude of the primer so only four independent parameters would

exist. However, two impulses are now available, bringing the total variables again to six. This exchange of independent parameters and number of constraint equations continues to the maximum number of impulses, namely six. Here, for six impulses no freedom is available with the five parameters. However, six impulse magnitudes are at our disposal allowing the use of six free variables. The problem is thus a very complex optimal transfer search problem and, even if a program were constructed to perform this search, a method of presentation of the solutions would be an almost impossible task. In this report, the problem to be analyzed is a sub-family of the much larger family of solutions to the general rendezvous problem. The sub-family will be discussed in detail in the next chapter.

Chapter III

ANALYSIS AND RESULTS

The sub-family to be analyzed is the family of solutions having Hamiltonians or primer histories symmetrical about some axis. This would indicate that the impulses are located symmetrically about this axis. It is further assumed that the impulse magnitudes are also symmetric about this axis. It will be shown that this corresponds to orbits having equal semi-major axes.

A. Analysis

Assume a symmetrical primer magnitude history such that

$$|\bar{\lambda}_v| = 1 \quad \text{at positions } \pm\theta_j \ (j = 1, 2 \ldots) \tag{3.1}$$

where the θ's are symmetrical relative to the mid-position $\theta = 0$. Also, assume that the impulses $|\overline{\Delta V}_j|$ are the same at both $+\theta_j$ and $-\theta_j$.

For symmetry:

$$\eta = 0 \quad \text{and} \quad \zeta = 0$$

or

$$\eta = 0 \quad \text{and} \quad \mu = 0 . \tag{3.2}$$

The symmetric primer for $\zeta = 0$ is

$$F(\theta_i) = (2\gamma + \cos\theta_i)^2 + (3\gamma\theta_i + 2\sin\theta_i)^2 + \mu^2 \cos^2\theta_i \tag{3.3}$$

and for $\mu = 0$

$$F(\theta_i) = (2\gamma + \cos\theta_i)^2 + (3\gamma\theta_i + 2\sin\theta_i)^2 + \zeta^2 \sin^2\theta_i . \qquad (3.4)$$

The radial impulse component, $2\gamma + \cos\theta_i$, is an even function of θ_i so that the impulse is directed in the same sense in the radial direction as indicated in Fig. 3 by impulse direction 1. The tangential component $3\gamma\theta_i + 2\sin\theta_i$ is an odd function so that the sense reverses, indicated by impulse direction 2 in Fig. 3. The net result is that the vacant focus is displaced in a direction perpendicular to the line of symmetry. This indicates that

$$\Delta a \equiv 0$$

$$\overline{\Delta e} \quad \text{is perpendicular to line of symmetry,} \quad \theta = 0 . \qquad (3.5)$$

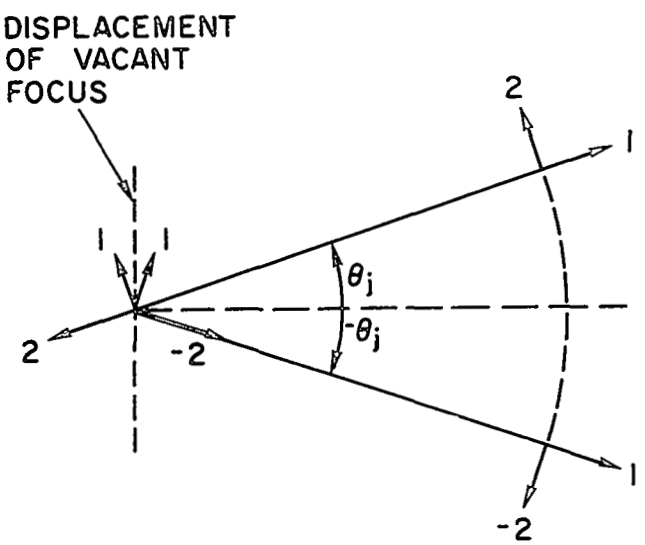

Fig. 3. EFFECT OF IMPULSES ON DISPLACEMENT OF VACANT FOCUS.

For $\zeta = 0$ the out-of-plane component is an even function so that the plane is rotated about the line of symmetry, that is, the line of symmetry is the line of nodes. The out-of-plane component for $\mu = 0$ is odd so that the plane is rotated about an axis perpendicular to the

line of symmetry. This indicates then that the line of symmetry is perpendicular to the line of nodes.

The transcendental equation for the maxima location for $\zeta = 0$ is

$$2\gamma\ \theta = \frac{-\sin\theta\left\{\frac{4}{3}\gamma + \left(1 - \frac{\mu^2}{3}\right)\cos\theta\right\}}{\frac{3\gamma}{2} + \cos\theta} \tag{3.6}$$

and for $\mu = 0$

$$2\gamma\ \theta = \frac{-\sin\theta\left\{\frac{4}{3}\gamma + \left(1 + \frac{\zeta^2}{3}\right)\cos\theta\right\}}{\frac{3\gamma}{2} + \cos\theta} \quad .$$

The reference orbit is chosen to be located symmetrically between the initial and final orbits as shown in Fig. 4

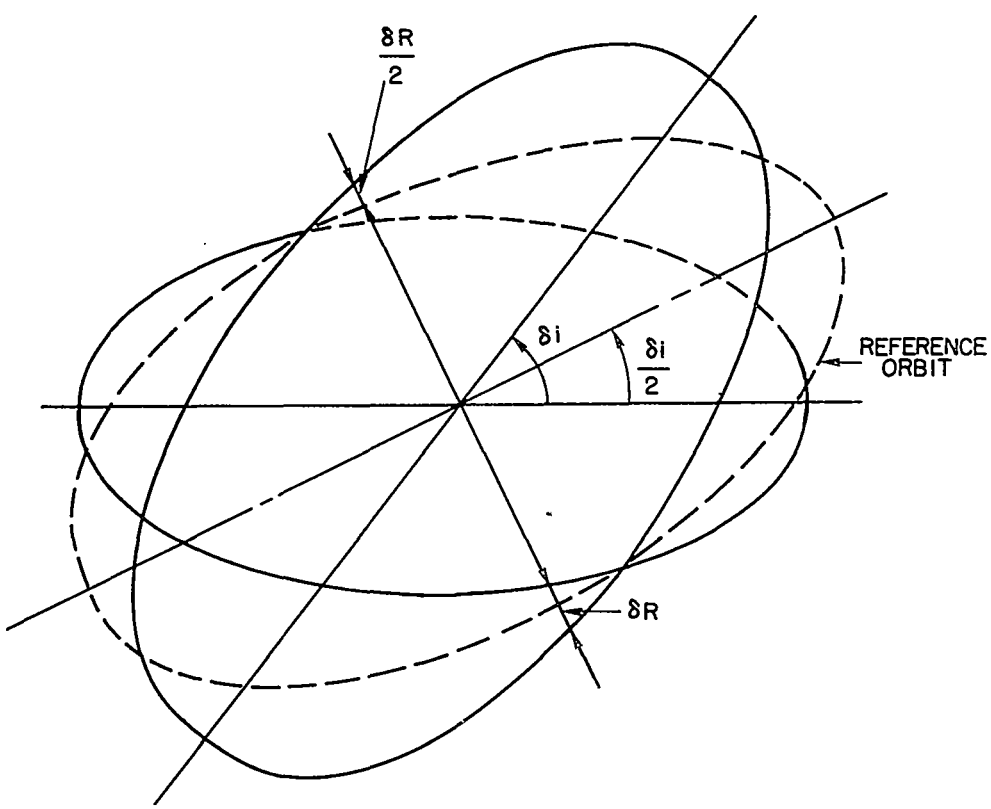

Fig. 4. REFERENCE ORBIT LOCATION.

B. Rendezvous Boundary Value Problem

The impulse locations for the primer defined by (3.3) or (3.4) are symmetric about the line of symmetry. Adjusting the integration constant t_p so that $\theta = 0$ along the line of symmetry a four-impulse symmetric primer would appear as in Fig. 5.

The symmetry allows the analysis to be rewritten as follows.

Let
$$t_* = \frac{t_f - t_i}{2} \tag{3.7}$$

so that

$$\begin{aligned} \theta_{fi} &= \theta_{fh} + \theta_{hi} \\ &= 2\theta_{fh} \\ &= -2\theta_{hf} \end{aligned} \tag{3.8}$$

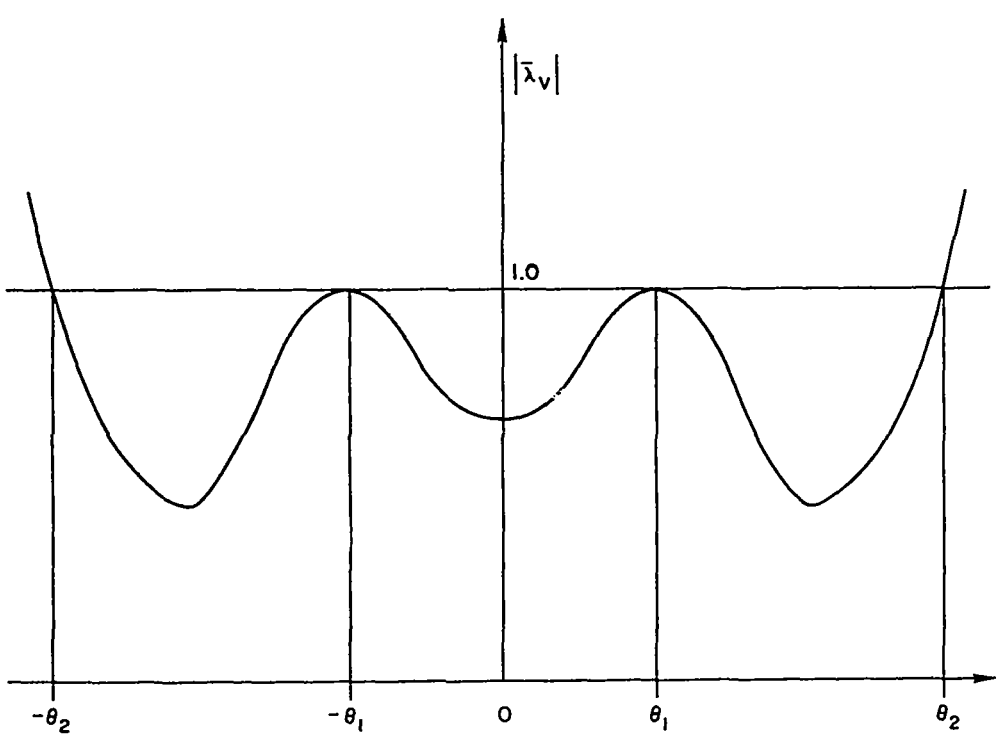

Fig. 5. FOUR-IMPULSE SYMMETRIC PRIMER.

where

$$\theta_{ij} = n(t_i - t_j) \ .$$

The states at time t_o can be written to first order; that is, for $\zeta = 0$

$$X(t_o) = \begin{bmatrix} -\frac{1}{2}\delta e \sin\theta_{hf} \\ -\delta e(1 - \cos\theta_{hf}) - \frac{\delta\theta_F}{2} \\ \frac{\delta i}{2}\sin\theta_{hf} \\ \frac{1}{2}\delta e \cos\theta_{hf} \\ \delta e \sin\theta_{hf} \\ -\frac{\delta i}{2}\cos\theta_{hf} \end{bmatrix} \tag{3.9}$$

and for $\mu = 0$

$$X(t_o) = \begin{bmatrix} -\frac{1}{2}\delta e \sin\theta_{hf} \\ -\delta_e(1 - \cos\theta_{hf}) - \frac{\delta\theta_F}{2} \\ \frac{\delta i}{2}\cos\theta_{hf} \\ \frac{1}{2}\delta e \cos\theta_{hf} \\ \delta e \sin\theta_{nf} \\ \frac{\delta i}{2}\sin\theta_{hf} \end{bmatrix} \tag{3.10}$$

where δe is the component of the eccentricity vector perpendicular to the line of symmetry. For example, for symmetry about the line of nodes

$$\delta e = \delta e_{\perp} \tag{3.11}$$

and for symmetry about a line perpendicular to the line of nodes

$$\delta e = \delta e_{\parallel} \ . \tag{3.12}$$

The state at time t_f, to first order for $\zeta = 0$ is

$$X(t_f) = \begin{bmatrix} -\frac{1}{2}\,\delta e \sin\theta_{hf} \\ \delta e(1 - \cos\theta_{hf}) + \frac{\delta\theta_F}{2} \\ \frac{\delta i}{2}\sin\theta_{nf} \\ -\frac{\delta e}{2}\cos\theta_{hf} \\ \delta e \sin\theta_{hf} \\ \frac{\delta i}{2}\cos\theta_{hf} \end{bmatrix} \tag{3.13}$$

and for $\mu = 0$

$$X(t_f) = \begin{bmatrix} -\frac{1}{2}\,\delta e \sin\theta_{hf} \\ \delta e(1 - \cos\theta_{hf}) + \frac{\delta\theta_F}{2} \\ -\frac{\delta i}{2}\cos\theta_{hf} \\ -\frac{\delta e}{2}\cos\theta_{hf} \\ \delta e \sin\theta_{hf} \\ \frac{\delta i}{2}\sin\theta_{hf} \end{bmatrix} \qquad (3.14)$$

From (3.13), (3.14), and the definition of $\Phi(t_h, t_j)$ and $X'(t_f)$ we obtain, for $\zeta = 0$,

$$X(t_h) = \begin{bmatrix} 0 \\ \delta\theta_F \\ -\delta e_\perp \\ 0 \\ \delta i \end{bmatrix}$$

and, for $\mu = 0$,

$$X(t_h) = \begin{bmatrix} 0 \\ \delta\theta_F \\ -\delta i \\ -\delta e_{11} \\ 0 \\ 0 \end{bmatrix} . \qquad (3.15)$$

The state equations can be rearranged so as to appear in the following form.

$$\delta e = -2 \sum_i \Delta V_i [\cos \theta_i (\lambda_u)_i + 2 \sin \theta_i (\lambda_v)_i]$$

$$\delta\theta_F' = \delta\theta_F + 2\delta e \cos \theta_f = 2 \sum_i \Delta V_i [3\theta_i (\lambda_v)_i - 2(\lambda_u)_i]$$

$$\delta i = 2 \sum_i \Delta V_i (\lambda_w)_i \cos \theta_i \qquad (3.16)$$

where

$$(\lambda_u)_i = \frac{1}{\sqrt{F(\theta_i)}} (2\gamma + \cos \theta_i)$$

$$(\lambda_v)_i = -\frac{1}{\sqrt{F(\theta_i)}} (3\gamma\theta_i + 2 \sin \theta_i)$$

$$(\lambda_w)_i = \frac{1}{\sqrt{F(\theta_i)}} \mu \cos \theta_i \qquad (3.17)$$

or

$$(\lambda_w) = \frac{1}{\sqrt{F(\theta_i)}} \zeta \sin \theta_i$$

where $F(\theta_i)$ is defined in (3.3) or (3.4). $\delta\theta_F'$ is introduced in this particular form to remove the dependence of $\delta\theta_F$ on $\theta(t_f)$ so that during a coast $\delta\theta_F'$ remains constant for a change in $\theta(t_f)$.

These equations, (3.16), are then used for the entire numerical analysis for both cases and for all impulse regions.

C. Maxima at $\theta = 0$

The assumption of symmetry of the magnitudes of the impulses is continued on into the investigation of five- and three-impulse type solutions. The symmetry of the primer would require a maximum to appear at $\theta = 0$. For a maximum the second derivative of $F(\theta)$ must be less than zero at $\theta = 0$.

For the case $\zeta = 0$, $\mu \neq 0$ and the second derivative is determined as

$$F''(\theta) = -\cos\theta(2\gamma + \cos\theta) + \sin^2\theta$$

$$- 2\sin\theta(3\gamma\theta + 2\sin\theta + (3\gamma + 2\cos\theta)^2$$

$$+ \mu^2\sin^2\theta - \mu^2\cos^2\theta < 0 \quad . \tag{3.18}$$

At $\theta = 0$ the condition is

$$9\gamma^2 + 10\gamma + (3 - \mu^2) < 0 \tag{3.19}$$

or

$$-\frac{5}{9} - \sqrt{9\mu^2 - 2} < \gamma < -\frac{5}{9} + \sqrt{9\mu^2 - 2} \quad . \tag{3.20}$$

For a real γ, μ^2 must be greater than 2/9. The conclusion is then that a symmetric three-impulse type primer exists for $\zeta = 0$.

For $\mu = 0$, $\zeta \neq 0$ and the second derivative is found to be

$$F''(\theta) = -\cos\theta(2\gamma + \cos\theta) + \sin^2\theta$$

$$- 2\sin\theta(3\gamma\theta + 2\sin\theta) + (3\gamma + 2\cos\theta)^2$$

$$+ \zeta^2\cos^2\theta - \zeta^2\sin^2\theta < 0 \quad . \tag{3.21}$$

At $\theta = 0$ the inequality criterion becomes

$$9\gamma^2 + 10\gamma + (3 + \zeta^2) < 0 \tag{3.22}$$

which is impossible for real γ and ζ. Thus for $\mu = 0$, $\zeta \neq 0$ a three-impulse type symmetric primer does not exist.

D. Various Impulse Solutions

It was found that for $\gamma \ll 1$ and $\mu^2 \simeq 3$, three and four equal maxima could be found. This suggests the possibility of five and six impulses as shown in Figs. 6 and 7. The analysis for both five and six impulses indicated the existence of such impulses for $\zeta = 0$ but not for $\mu = 0$. Thus, as shown for the existence of maxima at $\theta = 0$, five and six impulses will occur for symmetry about the line of nodes but not for symmetry about an axis perpendicular to the line of nodes. Further numerical analysis showed that the total transfer angle for five impulses close to 4π, 12π, etc., and for six impulses is 8π, 16π, etc. The existence of six impulses agrees with Marec [29] in that they appear for very small δa and for line of symmetry near the line of nodes. Here $\delta a = 0$ and line of nodes is the line of symmetry, and the total transfer time is almost an integral number of revolutions, here found to be four revolutions, eight revolutions, etc.

For a symmetric primer with impulses of symmetric magnitude a two-impulse-plus-coast region will exist only adjacent to the boundary of a four-impulse region. This is true, since the regions requiring an initial or final coast require that either the initial or final impulse magnitude of a neighboring region go to zero. Since the impulse magnitudes are assumed to be symmetric here, both initial and final impulse

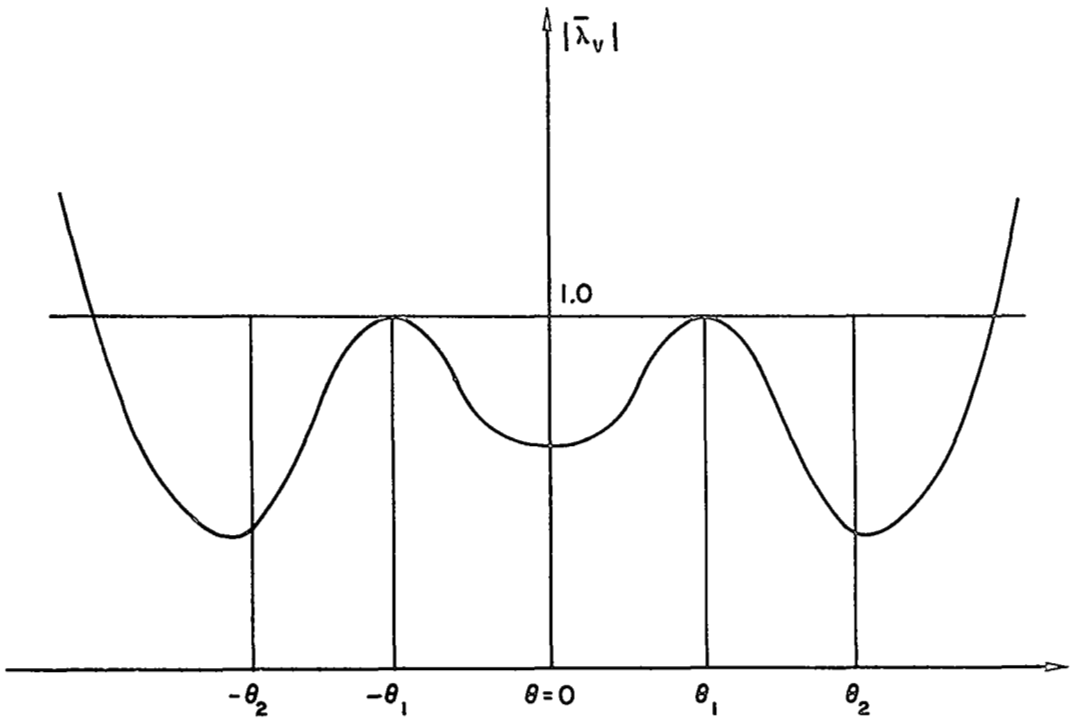

Fig. 6. TWO-PLUS-COAST PRIMER.

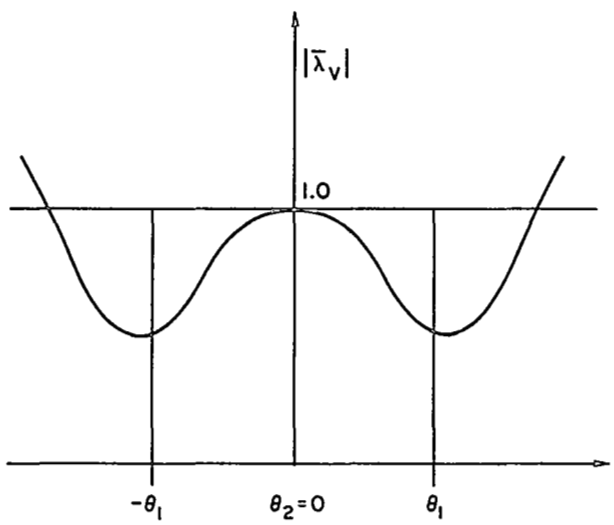

Fig. 7. ONE-PLUS-COAST PRIMER.

magnitudes go to zero simultaneously. For the symmetric primer the two-impulse-plus-coast primer magnitude will appear as in Fig. 8. Impulses occur at $\pm\theta_1$ and rendezvous begins at $-\theta_2$ and terminates at θ_2 with initial and final coast.

A two-impulse-plus-coast region will exist in both cases under investigation.

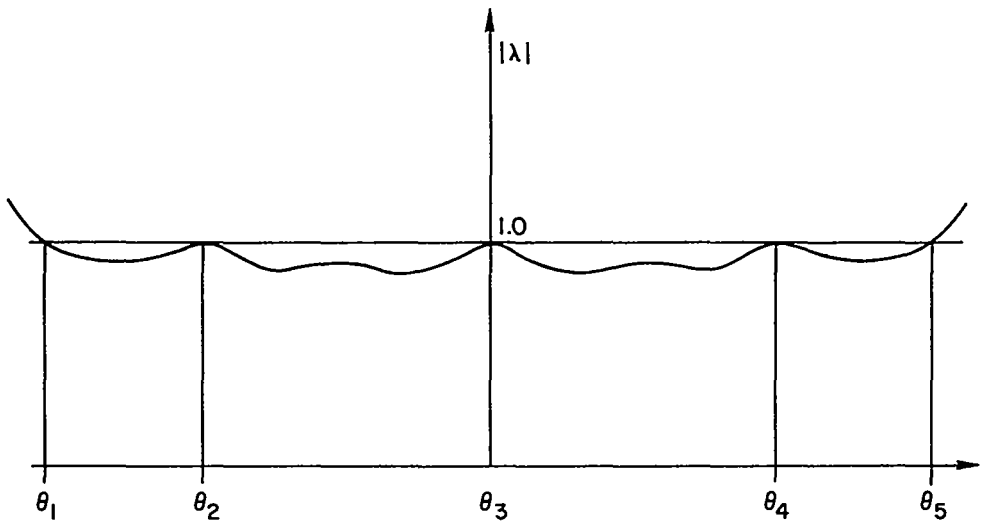

Fig. 8. FIVE-IMPULSE PRIMER HISTORY.

A one-impulse-plus-coast region will occur adjacent to the symmetric three-impulse region in the case of symmetry about the line of nodes. This region occurs when the initial and final impulses vanish simultaneously in the three-impulse region. A typical primer magnitude is shown in Fig. 9 for the one-plus-coast solution. One impulse at $\theta = 0$ with initiation of rendezvous at θ_1 and termination at θ_1.

Once the existence of a five- or six-impulse Hamiltonian has been determined, the corresponding range of rendezvous parameters is easily determined. With the availability of a five-and six-impulse region a three-plus-coast region, adjacent to the five-impulse region, and a four-plus-coast region, adjacent to the six-impulse region, are also present.

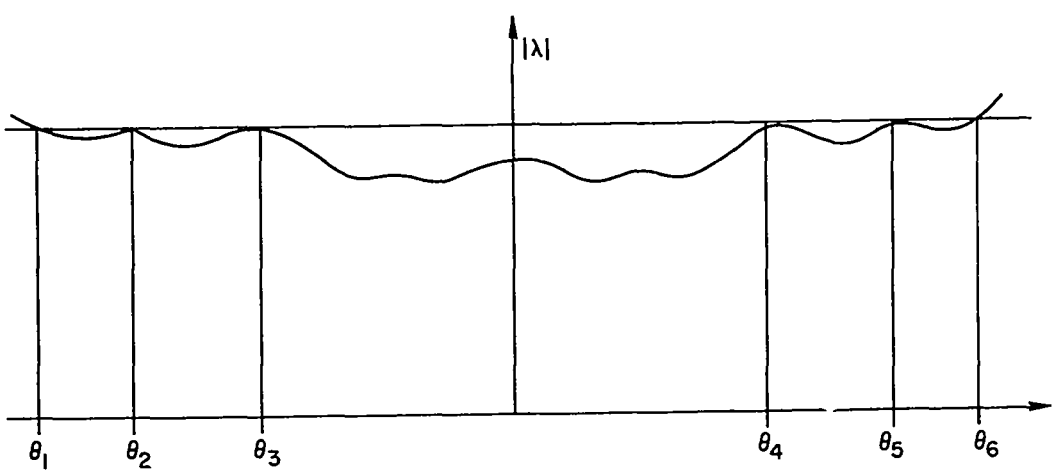

Fig. 9. SIX-IMPULSE PRIMER HISTORY.

E. Non-Unique Solutions

This section investigates a set of multiple-impulse solutions for which the maximum principle is degenerate. This occurs when the magnitude of the primer is unity during the entire transfer. Although this solution satisfies the necessary conditions for an optimal transfer, the impulse times are not determined by the maximum principle. This behavior is analogous to the singular arc which arises in nonlinear problems when the switching function is zero over a finite time interval.

Equation (3.3) shows that in order to have a primer of constant magnitude, for the case $\zeta = 0$,

$$\gamma = 0$$

$$\mu = \sqrt{3} \ , \tag{3.23}$$

For $\mu = 0$ a non-unique primer cannot be obtained. From (2.8) and (2.33) solutions with $\gamma = 0$ represent solutions from which the time constraint does not affect the cost, that is, the cost is that of time-free transfer.

Introducing the paramater α defined by

$$\alpha = \tan^{-1} \frac{\delta i}{\delta e_{\perp}} \tag{3.24}$$

allows the following analog between non-unique solutions and the transfer problem. For $\alpha < 60^{\circ}$ the corresponding transfer region is Region I, defined in [30] as the degenerate region. Here the associated cost from [30] is

$$\tau = \delta e + \sqrt{3}\delta i \ . \tag{3.25}$$

To achieve this cost from (3.16), $\gamma = 0$ and $\mu = \sqrt{3}$ the conditions required for non-unique solutions.

It is possible to obtain non-unique solutions for symmetry about the line of nodes and for $\alpha < 60°$ but not for symmetry about a line perpendicular to the line of nodes or for $\alpha > 60°$.

The boundaries of the non-unique region are determined from the second equation of (3.16). For a given α, the maximum and minimum values of $\delta\theta_F'/\tau$ are found. This may be accomplished graphically as follows.

$$\delta e = 2 \sum_i \frac{\Delta V_i}{\sqrt{F(\theta_i)}} (4 - 3 \cos^2 \theta_i)$$

$$\delta\theta_F' = -2 \sum_i \frac{\Delta V_i}{\sqrt{F(\theta_i)}} (6\theta_i \sin \theta_i + 2 \cos \theta_i)$$

$$\delta i = 2 \sum_i \frac{\Delta V_i}{\sqrt{F(\theta_i)}} \quad 3 \cos^2 \theta_i \cdot \tag{3.26}$$

For a given $\delta i/\delta e = \tan \alpha$, $\alpha < 60°$, the maximum and minimum values of ω, defined as

$$\omega = \tan^{-1} \frac{\delta\theta_F'}{\sqrt{\delta e^2 + \delta i^2}} \tag{3.27}$$

must be determined. From (3.26) obtain

$$\cot \alpha = \frac{|\delta e|}{\delta i} = \frac{4 - 3 \text{ ave } \cos^2 \theta_i}{\sqrt{3} \text{ ave } \cos^2 \theta_i} \tag{3.28}$$

or

$$\sum_i W_i \cos^2 \theta_i = \text{ave} \cos^2 \theta_i = \frac{4}{3 + \sqrt{3} \cot \alpha} < 1 \quad . \qquad (3.29)$$

So that the problem is to determine

$$\max_{\min} \sum_i W_i (3\theta_i \sin \theta_i + \cos \theta_i) \qquad (3.30)$$

subject to

$$\sum_i W_i = 1, \quad \text{ave} \cos^2 \theta_i = \frac{4}{3 + \sqrt{3} \cot \alpha} \quad . \qquad (3.31)$$

Therefore, plotting $3\theta \sin \theta + \cos \theta$ vs $\sin^2 \theta$ yields a graphical method to perform the computation. Such a plot is shown in Fig. 10. The maximum and minimum values of (3.30) can be obtained by constructing the convex hull corresponding to a given $\theta(t_f)$. Figure 10 shows the convex hull, heavy lined portion, for $\theta(t_f) = 225°$. For ave $\cos^2 \theta_i = 0.7$, or ave $\sin^2 \theta_i = 0.3$, the maximum value of $3\theta \sin \theta + \cos \theta$ is read off on the chart as being equal to 3.4 and corresponds to a two-plus-coast transfer, and the minimum is read at -7.0 which also corresponds to a two-plus-coast transfer. It can be seen that the convex hull is a function of $\theta(t_f)$ and that for ω's corresponding to points inside this hull it is possible to determine various non-unique optimal solutions. Two, two-plus-coast, three- and four-impulse solutions are possible.

F. Optimal Solutions Symmetric About the Line of Nodes

To obtain the impulse region boundaries one of the impulses in (3.16) is set to zero and the other impulses then varied until the desired value of α and the corresponding value of ω are obtained. The inverse of Eqs. (3.16) is then solved for the impulse magnitudes in terms of δe, $\delta\theta_F'$, and δi in order to determine the type of region that lies to

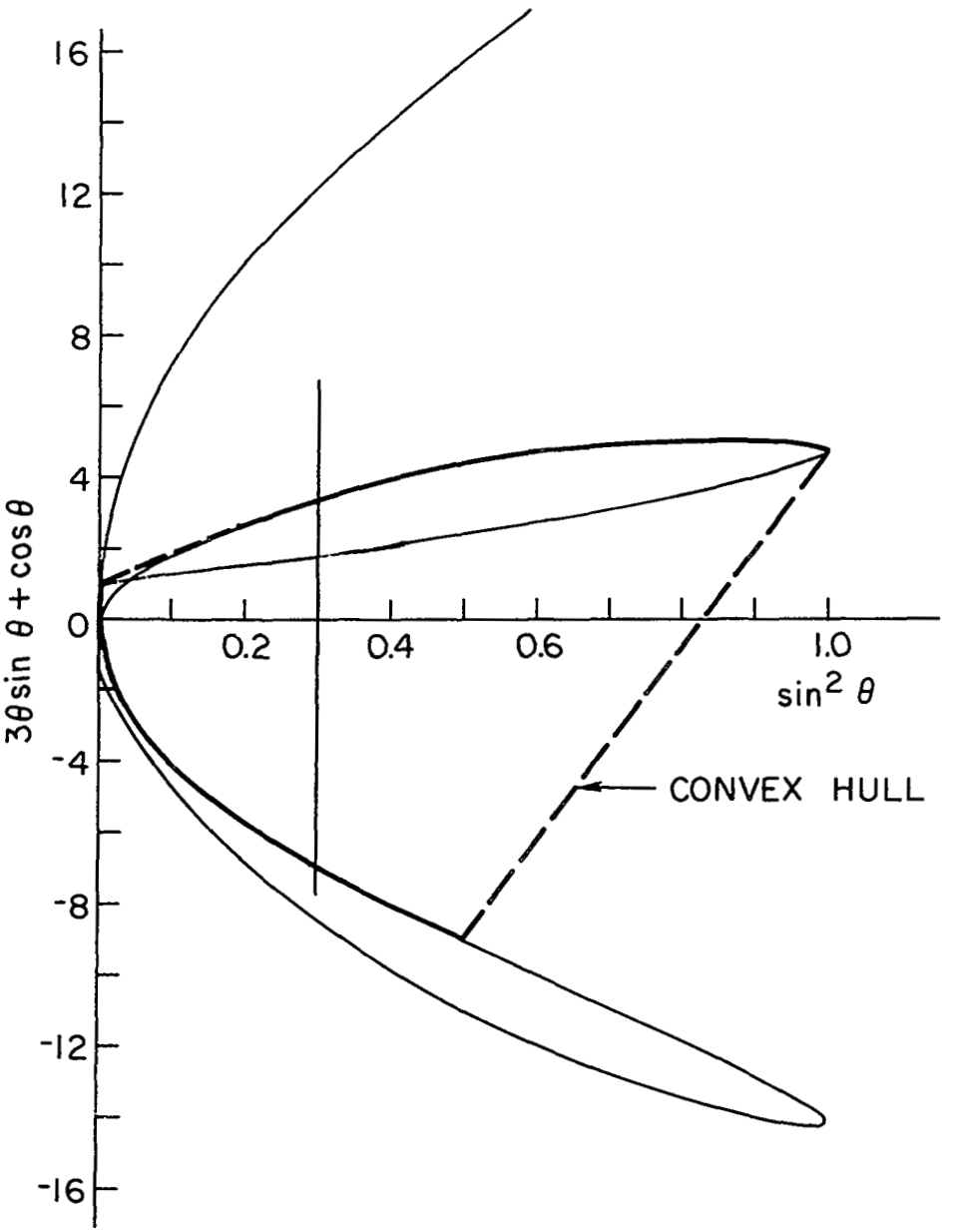

Fig. 10. $3\theta \sin\theta + \cos\theta$ VS $\sin^2\theta$.

either side of the boundary. Plots are then obtained for various $\alpha = \tan^{-1} \delta i/\delta e$ with ω vs t_f the total transfer time.

Figures 11 through 21 show such plots for

$$0° \leq \alpha \leq 90°. \tag{3.32}$$

In Fig. 11 the four impulse regions near $t_f = 2.0$ and 4.0 are bounded by a two-plus-coast region on the left and a two-impulse region on the right. The two-impulse region boundary is determined when the intermediate impulses of the four-impulse region vanish and the two-plus-coast region boundary is determined when the initial and final impulses vanish. The two-impulse boundaries are determined in like manner for the four-impulse region near $t_f = 0.5$ and 2.5. The three-four impulse boundary is determined as the impulse location of the intermediate impulses approaches zero. The two-three impulse boundary is determined when the impulse at $\theta = 0$ in the three-impulse region vanishes.

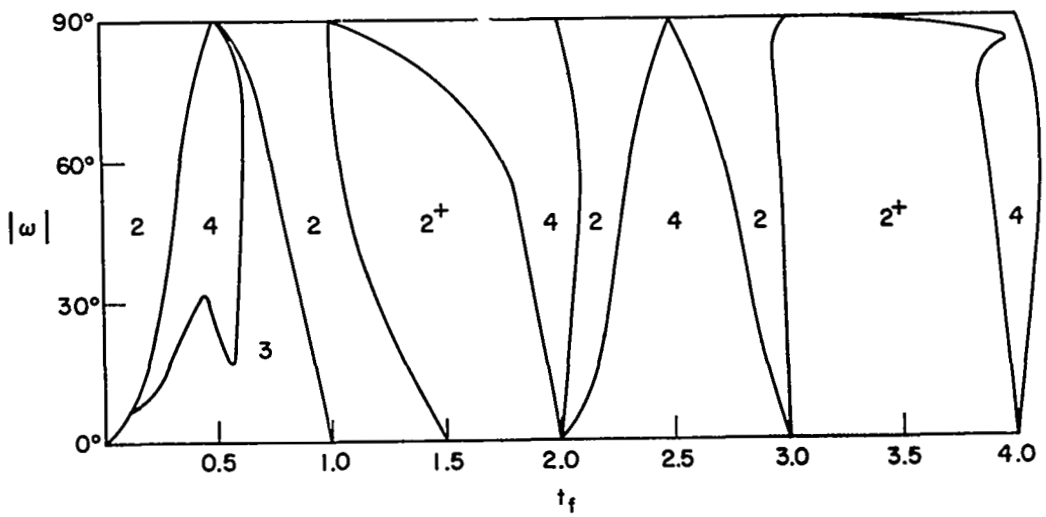

Fig. 11. IMPULSE REGIONS FOR $\alpha = 90°$,

For $\alpha = 85°$ a two-plus-coast region appears in the lower portion of the plot. All other regions are somewhat distorted forms of those for $\alpha = 90°$ and continue to appear as α decreases.

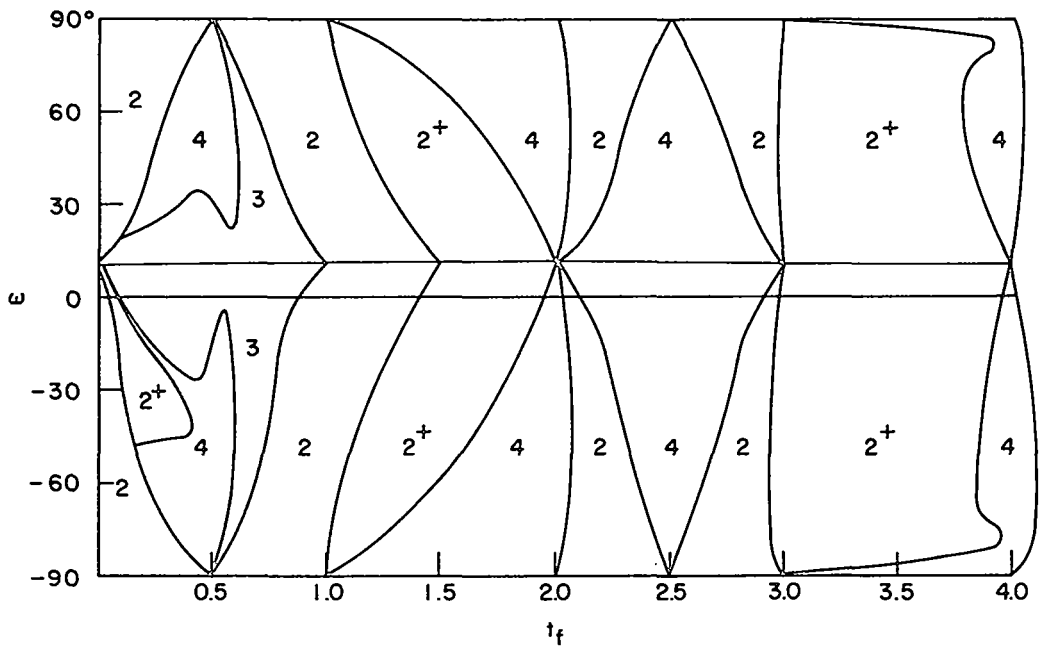

Fig. 12. IMPULSE REGIONS FOR $\alpha = 85°$.

For $\alpha = 68.7°$ a six- and a four-plus-coast region appear near $t_f = 4.0$. The two-plus-coast region near $t_f = 0$ has moved upwards and is stretched to the right. The end of the four-plus-coast region appears for $\alpha = 65°$. Beyond this value of α the four-plus-coast no longer appears. For $\alpha = 63.8°$ a five- and a three-plus-coast region appear near $t_f = 2.0$. The five- and three-plus coast and six-impulse regions have reached their limit at $\alpha = 60.8°$.

For $\alpha = 45°$ the non-unique region appears as shown in Fig. 19. The coplanar case, corresponding to $\alpha = 0°$, is shown in Fig. 21. As α approaches $0°$ the intermediate impulses of the four-impulse regions near $t_f = 0.5$ and 2.5 are located at $\theta = 90°$ and $270°$ respectively, and their magnitudes approach zero so that at $\alpha = 0°$ the two-impulse region is actually the boundary of the four-impulse region.

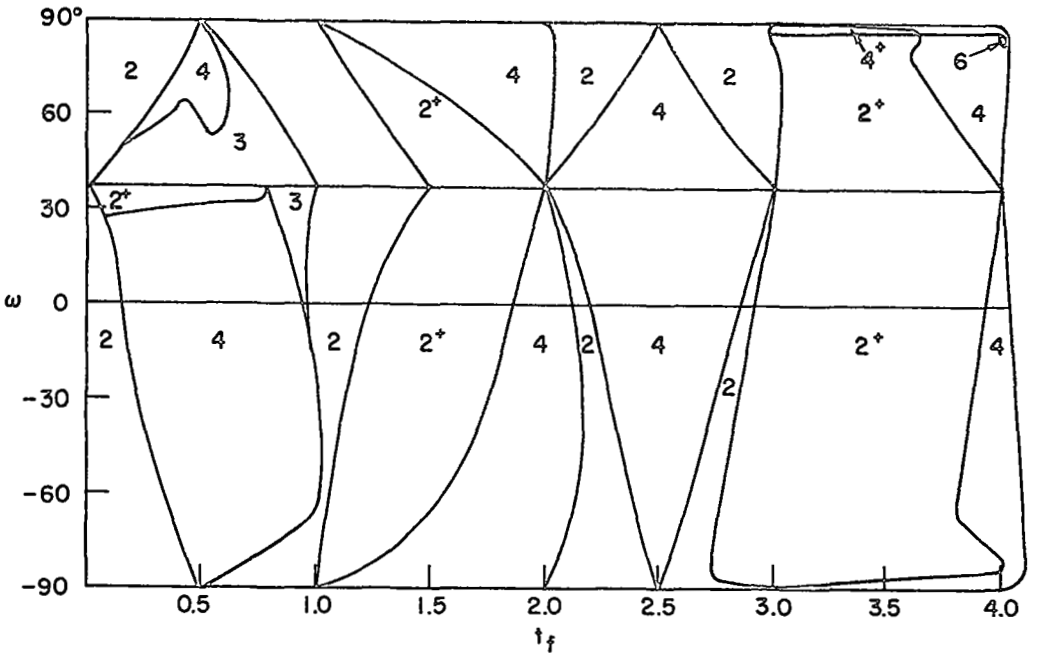

Fig. 13. IMPULSE REGIONS FOR $\alpha = 68.7°$.

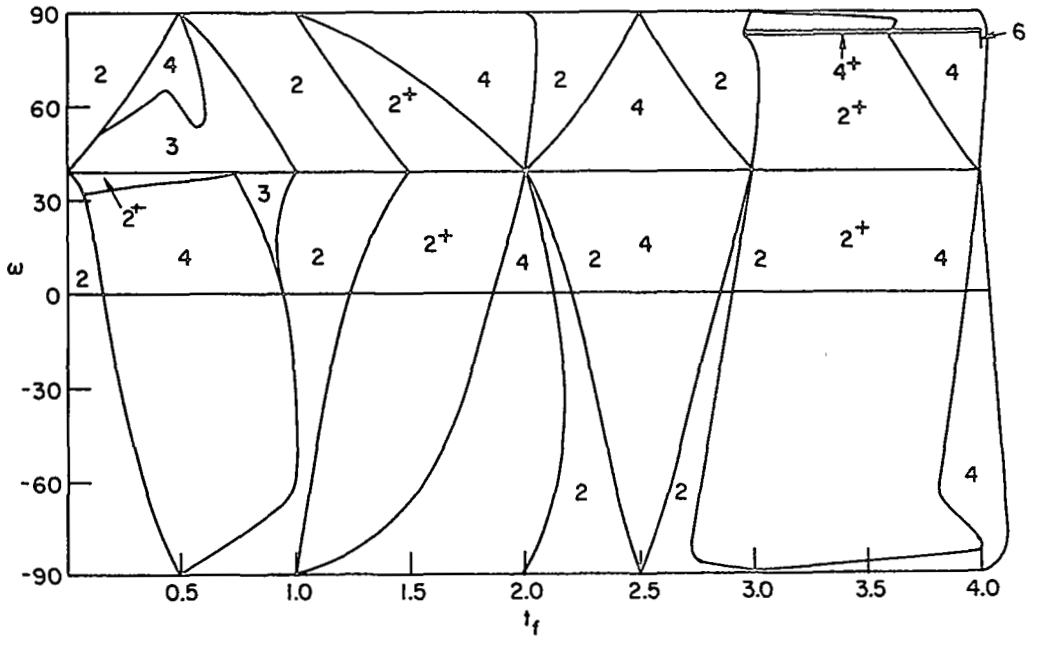

Fig. 14. IMPULSE REGIONS FOR $\alpha = 67°$.

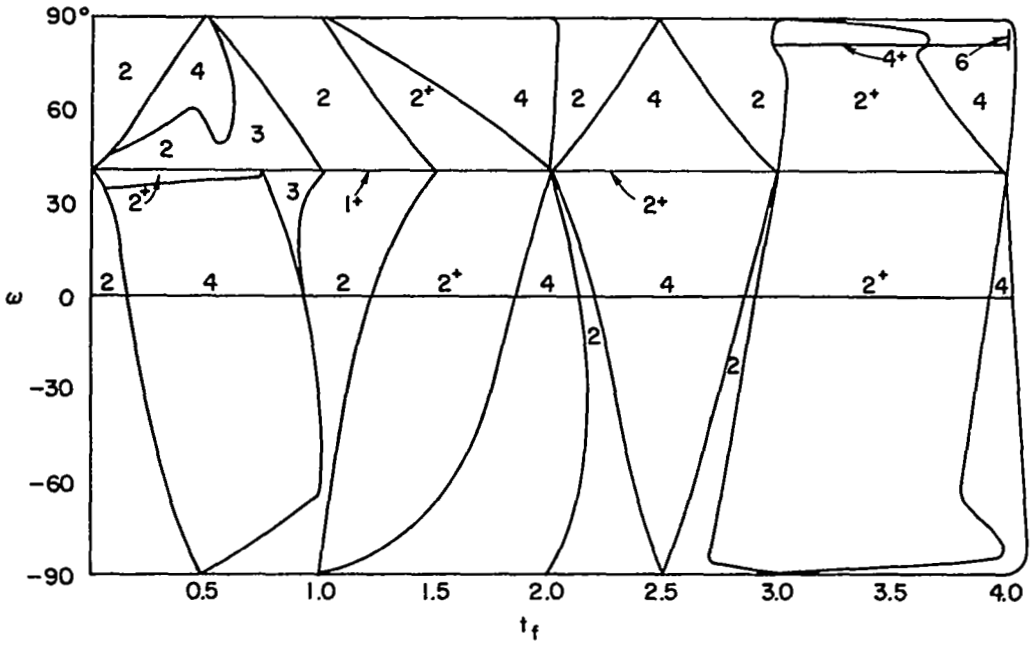

Fig. 15. IMPULSE REGIONS FOR $\alpha = 65°$.

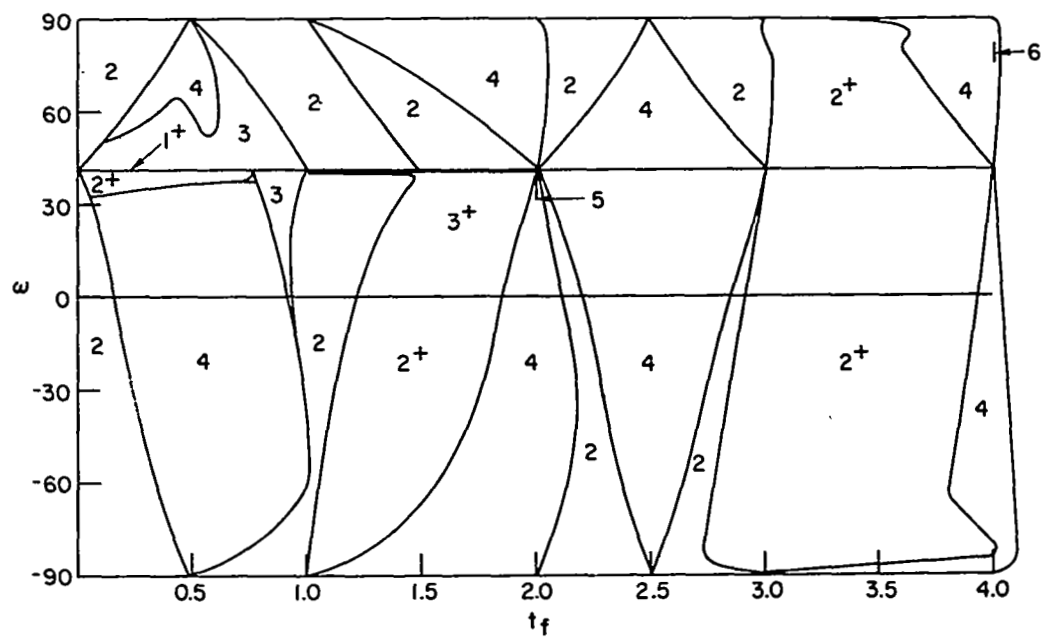

Fig. 16. IMPULSE REGIONS FOR $\alpha = 63.8°$.

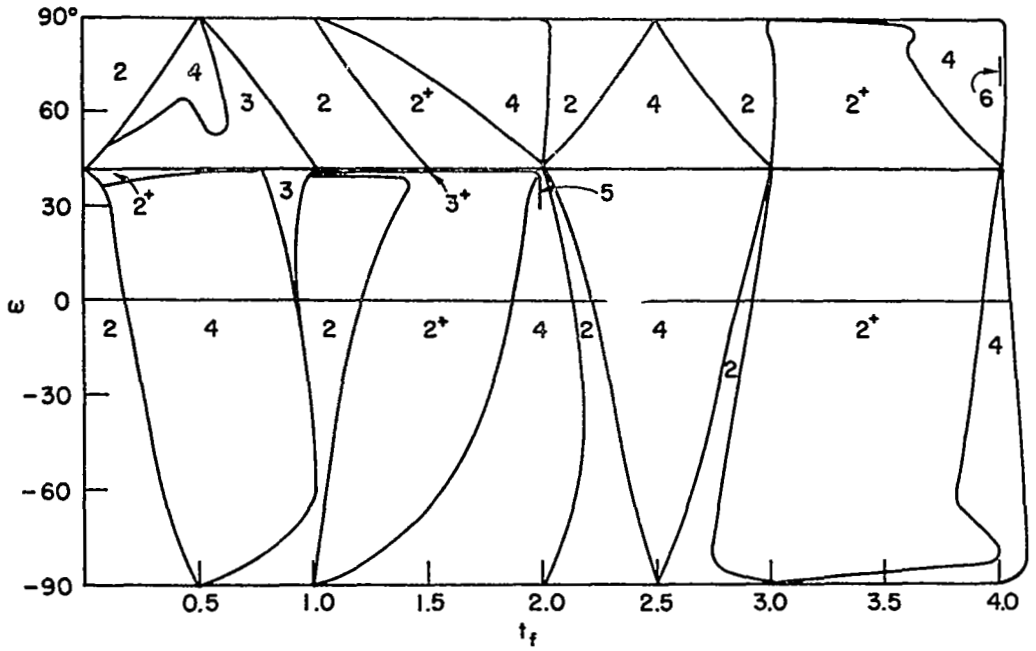

Fig. 17. IMPULSE REGIONS FOR $\alpha = 61.5°$.

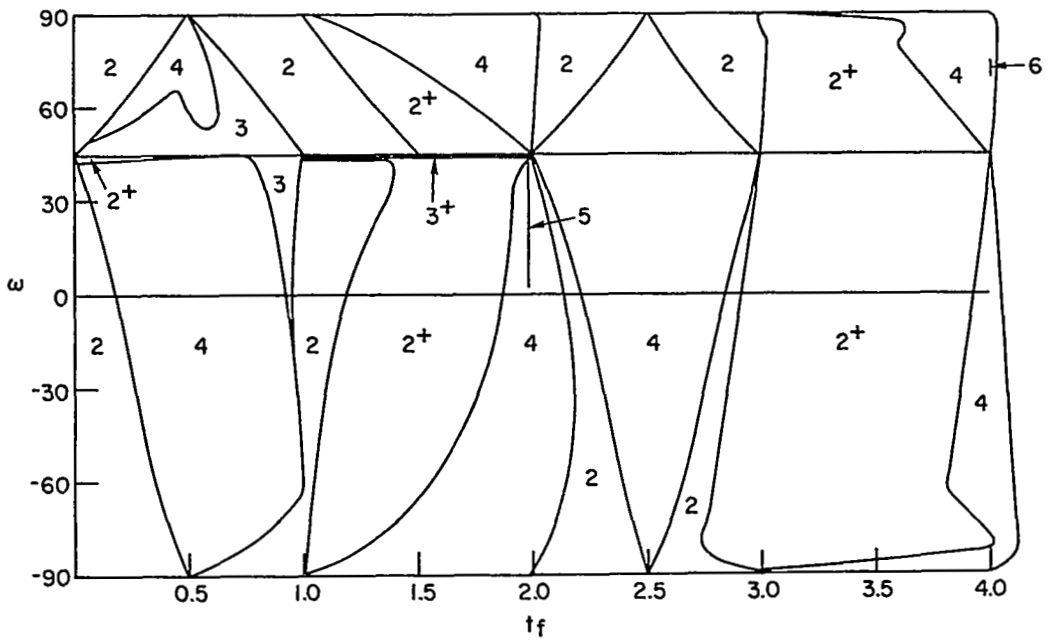

Fig. 18. IMPULSE REGIONS FOR $\alpha = 60.8°$.

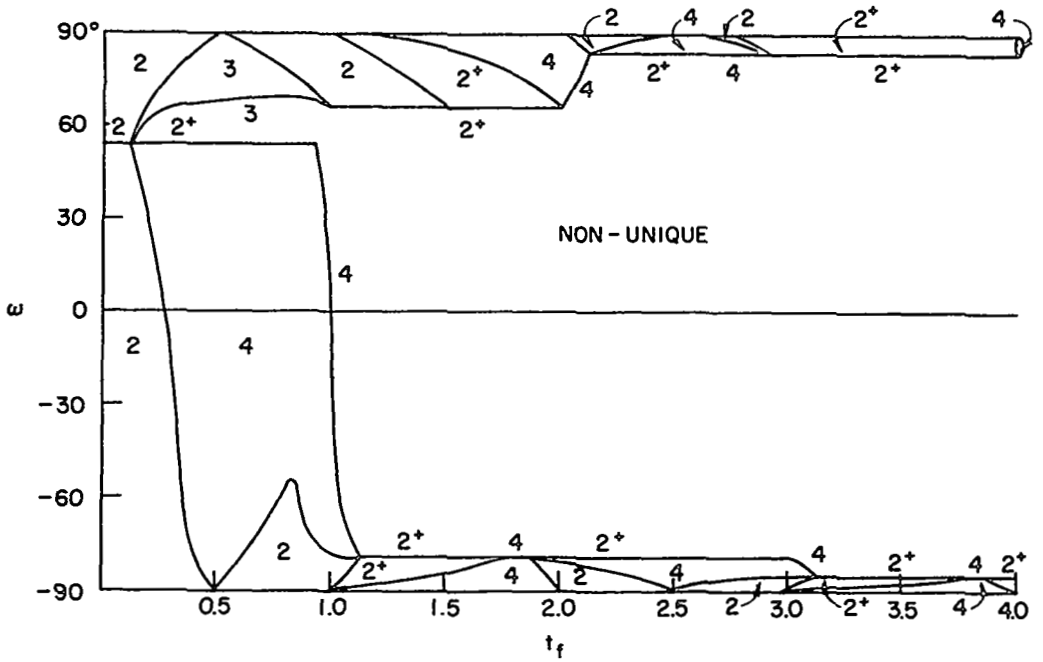

Fig. 19. IMPULSE REGIONS FOR $\alpha = 45°$.

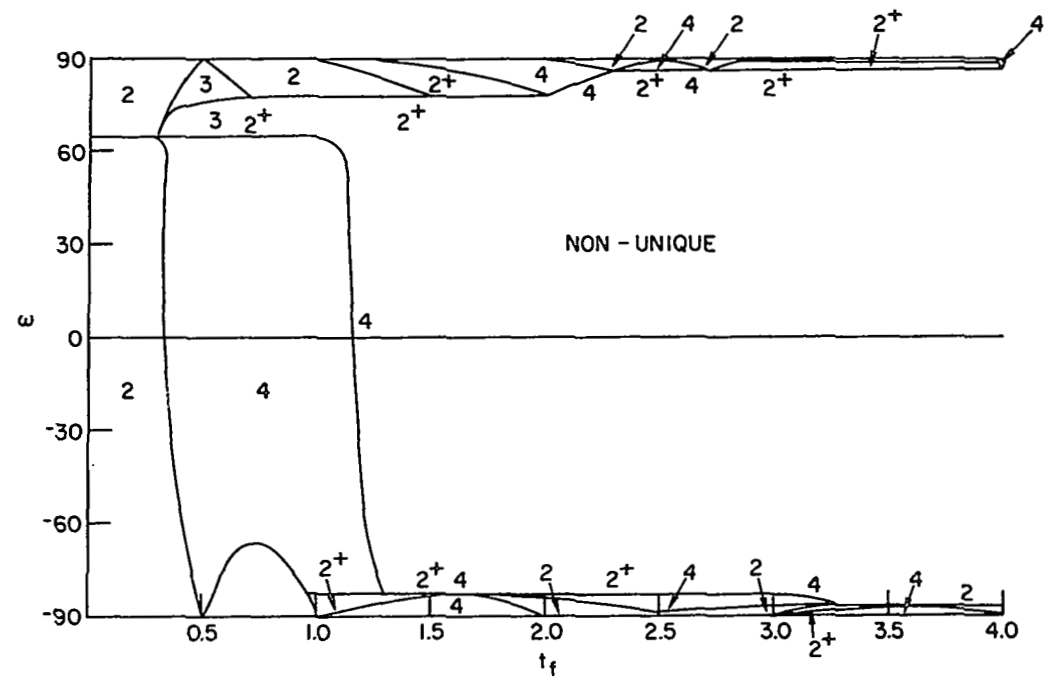

Fig. 20. IMPULSE REGIONS FOR $\alpha = 10°$.

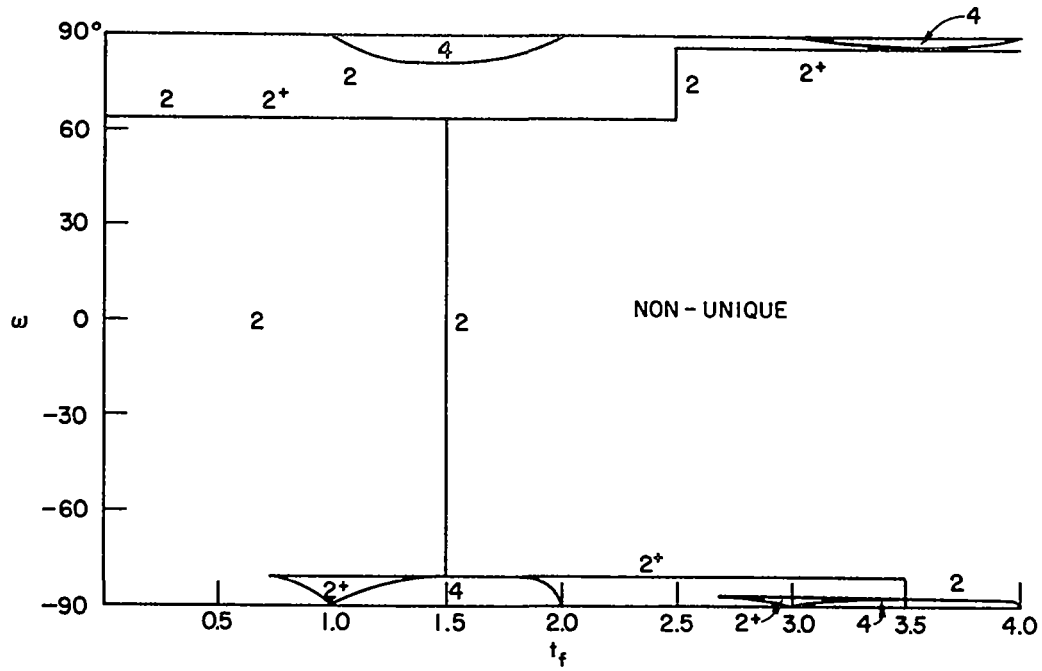

Fig. 21. IMPULSE REGIONS FOR $\alpha = 0°$.

Since the line of nodes is undefined in the coplanar problem, Fig. 21 holds true both for symmetry about the line of nodes and symmetry about a line perpendicular to the line of nodes.

To obtain negative α's the impulse directions in the plane of the orbit are reversed, that is, the signs of $(\lambda_u)_i$ and $(\lambda_v)_i$ are reversed. The effect of such a sign change is to reverse the sign of ω without affecting the sign of δi. Thus to obtain the optimal impulse strategies for negative α merely reverse the sign of α and ω simultaneously. Figures 3 through 13 yield a three-dimensional picture in parameter space of the optimal impulse strategies for

$$-90° < \alpha < 90°$$

$$-90° < \omega < 90° \qquad (3.33)$$

as functions of total transfer time t_f, measured in revolutions.

Enlargements of typical five- and six-impulse regions are shown in Figs. 22 and 23.

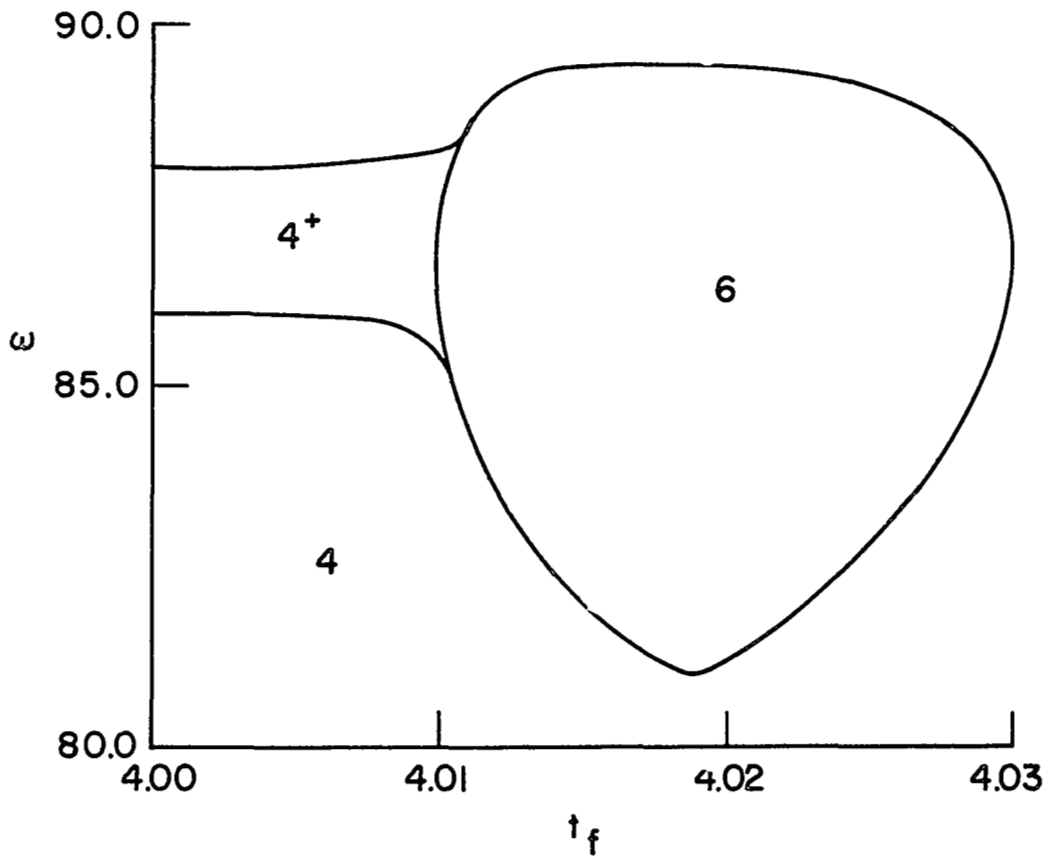

Fig. 22. ENLARGEMENT OF SIX-IMPULSE REGION FOR $\alpha = 65°$.

For $\alpha > 60°$ the time-free transfer solutions, that is $\gamma = 0$, lie in Region II defined in [30]. Region II is the non-degenerate region, and the cost associated with this region is

$$\tau = \sqrt{(\delta e_\perp)^2 + (\delta i)^2}. \tag{3.34}$$

From Eqs. (3.16) it is possible to achieve this cost from unique Hamiltonians. The solutions appear on the horizontal line displaced from $\omega = 0$. For $t_F < 1.0$ a one-plus-coast strategy is required located at

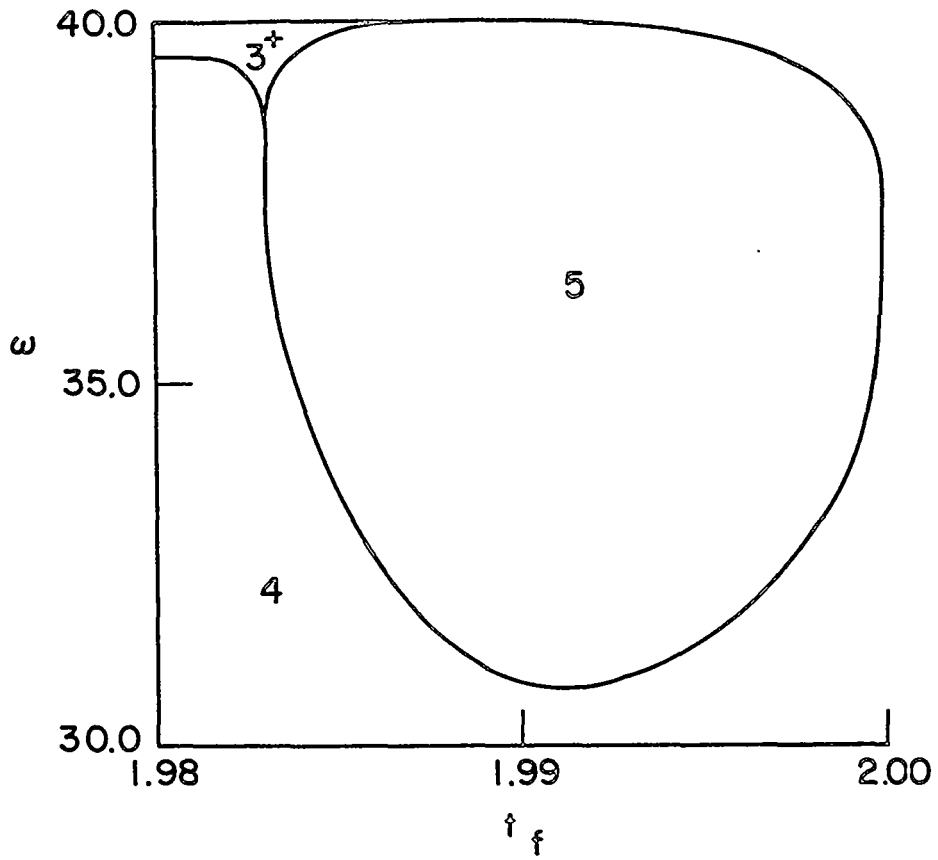

Fig. 23. ENLARGEMENT OF FIVE-IMPULSE REGION FOR $\alpha = 63.8°$.

$\theta = 0$. For $t_F > 1.0$ the impulse at $\theta = 0$ can be supplemented with impulses at $\theta = \pm 2\pi$. However, the cost is still given by (3.34). That is, for $t_F > 1.0$ the strategies are not unique since a mixture of strategies can be used with the same cost.

G. Optimal Solutions Symmetric About a Line Perpendicular to the Line of Nodes

The same type of analysis is used here as in Section III.F. except δe_{11} is substituted for $\delta e_{\perp}$ and now

$$\lambda_\omega = \zeta \sin \theta \ . \tag{3.35}$$

Figures 24 and 25 show the results of the numerical analysis. The parameter space is broken up into mainly two- and four-impulse regions. A two-plus-coast region does appear between $t_f = 0.5$ and $t_f = 1.5$. Figure 25 shows the optimal impulse regions for $\alpha \approx 65°$. Non-unique solutions do not exist here, and other charts would appear much like Fig. 25. Again for $\alpha < 0$ the sign of ω is reversed simultaneously.

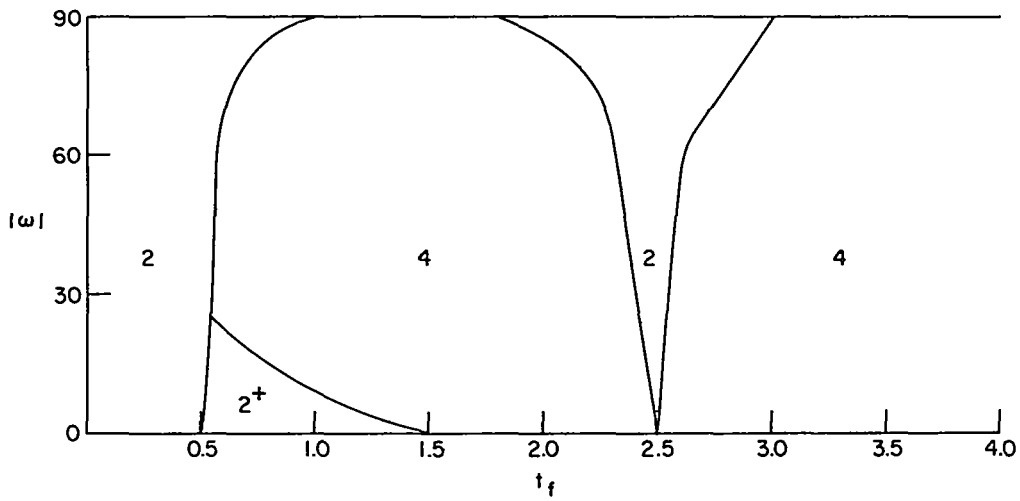

Fig. 24. IMPULSE REGIONS FOR $\mu = 0$ AND $\alpha = 90°$.

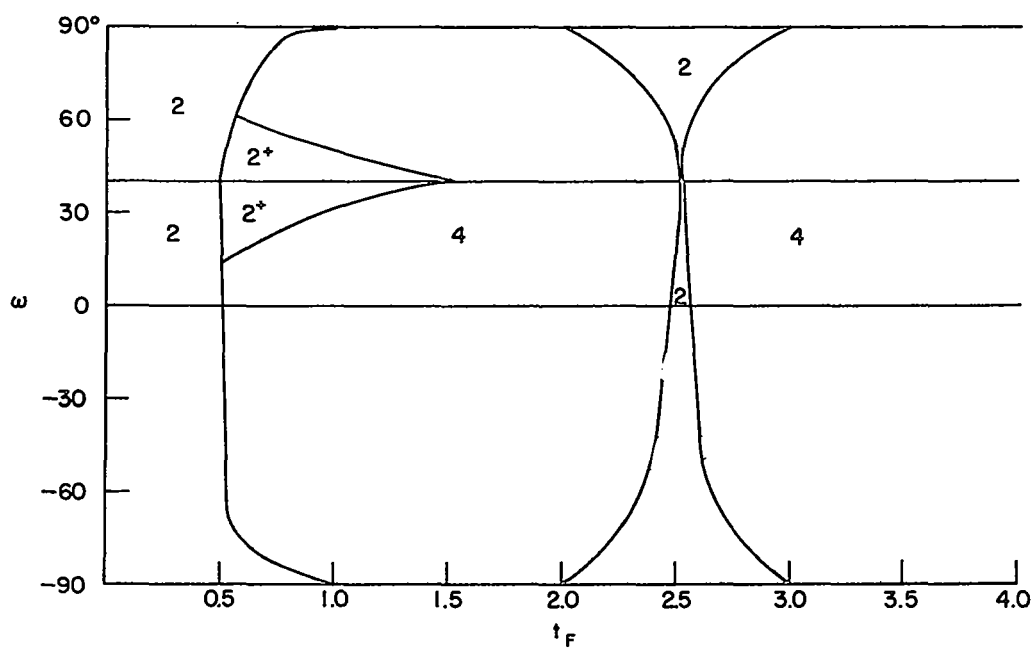

Fig. 25. IMPULSE REGIONS FOR $\mu = 0$ AND $\alpha = 65°$.

Chapter IV

CONCLUSIONS

The time-fixed problem has been investigated for the case of transfer between non-coplanar nearly circular equi-energy orbits with symmetry of impulse magnitude and location about the line of nodes or about a line perpendicular to the line of nodes. Charts are given which show the one, two, three, four, five, and six impulse regions characteristic of these cases.

This study should be extended to attempt a classification in three dimensions of the optimal number of impulses for other cases of near-circular rendezvous. This classification would be very valuable as input to an iterative optimization program for n-impulse interplanetary trajectories. An effort should be made to determine a suitable way of categorizing the optimal solutions to display the impulse times, magnitude, and directions for all the relevant initial conditions and transfer times.

REFERENCES

1. Hohmann, W., Die Erreichbarkeit der Himmelskoerper, R. Oldenburg, Munich (1925).

2. Lawden, D. F., "Interplanetary Rocket Trajectories," Advances in Space Science 1, ed. by F. I. Ordway III, Academic Press, New York (1959).

3. Lawden, D. F., Impulsive Transfer Between Elliptical Orbits, Optimization Techniques, ed. by G. Leitmann, Academic Press, New York (1962).

4. Lawden, D. F., Optimal Trajectories for Space Navigation, Butterworths, London (1963).

5. Hoelker, R. F. and R. Silber, "The Bi-elliptical Transfer Between Coplanar Circular Orbits," Proc. 4th Symposium on Space Technology, Los Angeles (1959).

6. Shternfeld, A., Soviet Space Science, Basic Books, Inc., New York, p. 109-111 (1959).

7. Edelbaum, T. N., "Some Extensions of the Hohmann Transfer Maneuver," ARS J 29, 864-865 (1959).

8. Marchal, C., "Transferts Optimaux entre Orbites Elliptiques" (Duree Indifferente), Proc. 16th. IAF Congress, Athens, Sep 1965.

9. Breakwell, J. V., "Minimum Impulse Transfer," Progress in Astronaut. and Aeronaut. 14 (1964).

10. Breakwell, J. V., "The Optimization of Trajectroies," SIAM J. 7, 2, Jun 1959.

11. Breakwell, J. V., "Minimum-impulse Transfer between a Circular Orbit and a Nearby Non-coplanar Orbit," Colloquim on Advanced Problems and Methods for Space Flight Optimization, Liege, Jun 1967.

12. Winn, C. B., "Minimum-fuel Transfers Between Coaxial Orbits, Both Coplanar and Non-coplanar," AAS Preprint 66-119, Jul 1966.

13. Marec, J. P., "Transfers Infinitesimaux Impulsionnels Economiques entre Orbites Quasi-circulaires non Coplanaires," Proc. 17th IAF Congress, Madrid, Oct 1966.

14. Edelabum, T. N., "Minimum Impulse Transfers in the Near Vicinity of a Circular Orbit," J. of Astronaut. Sci. XIV, 2, March-April 1967.

15. Kuzmak, G. E., "Optimal Multi-pulse Flight Between Close Quasi-circular non-coplanar Orbits," Translated from Kosmicheskie Issledovaniya, Vol. 5, No. 5, pp. 703-714, Sept-Oct, 1967.

16. Eckel, K., "Numerical Solutions of Non-coaxial Optimum Transfer Problems," J. of Astronaut. Sci. X, 3, Fall 1963.

17. Lion, P. M. and M. Handelsmann, "The Primer Vector of Fixed-time Impulsive Trajectories," AIAA Fifth Aerospace Sciences Meeting, New York, Jan 1967.

18. Marec, J. P., "Rendez-vous Impulsionnels Optimaux de Longue Duree entre Orbites Quasi-circulaires Proches, Coplanaires ou Non," Colloquium on Advanced Space Problems and Methods for Space Flight Optimization, Liege, Jun 1967.

19. Doll, J. R. and F. W. Gobetz, "Three-impulse Interplanetary Rendezvous Trajectories," presented at AAS Symposium, Huntsville, Ala. (1966).

20. Gobetz, F. W. and J. R. Doll, "How to Open a Launch Window," AAS Preprint 68-095, Sep 1968.

21. Prussing, J. E., "Optimal Multiple-impulse Orbital Rendezvous," TE-20, MIT (1967).

22. Kolbe, O. and P. Sagirow, "Die Strenge Optimal Loesung eines Speziellen Rendezvous Problems," Z. Flugwiss. 16. Jahrgang, Heft 4, Apr 1968.

23. Marinescu, A., "Untersuchung des Optimalen Rendezvous-Manoevers von Raumfahrzeugen auf Kreisbahnen Minimalen Treibstoffverbrauch," Z. Flugwiss. 16. Jahrgang, Heft 4, Apr 1968.

24. Marchal, C., J. P. Marec, and C. B. Winn, "Synthese des Resultats Analytiques sur les Transferts Optimaux entre Orbites Keplerienes," presented at XVIII^{e} Congres International d'Astronautique, Belgrade, Sep 1967.

25. Robinson, A. C., "A Survey of Methods and Results in the Determination of Fuel-optimal Impulsive Space Maneuvers," AAS Preprint 68-091, Sept 1968.

26. Melbourne, W. G. and C. G. Sauer, Jr., "Optimum Interplanetary Rendezvous with Power-limited Vehicles," AIAA J. 1, 1, Jan 1963.

27. Neustadt, L. W., "Optimization, A Moment Problem and Nonlinear Programming," SIAM J. on Control 2 (1964).

28. Stern, R. G. and J. E. Potter, "Optimization of Midcourse Velocity Corrections," IFAC Symposium on Automatic Control in the Peaceful Use of Space, Stavanger, Norway (1965).

29. Marec. J. P., "Contribution A L'etude des Rendez-vous, Multi-impulsionnels Optimaux, de Duree Moyenne, entre Orbites Quasi-circularies, Proches, Non-coplanaires," presented at 2e Colloque International sur les Methodes d' Optimisation. Akademgorodek, U.S.S.R., 20-26 Jun 1968.

30. Heine, W., "Researches In Optimal Transfer", SUDAAR Report No. 381, Jun 1969.

NASA-Langley, 1970 —— 30 CR-1508